Journal of
Synchrotron
Radiation

ISSN 1600-5775

Received 28 July 2014
Accepted 9 January 2015

Comparative study of the X-ray reflectivity and in-depth profile of a-C, B_4C and Ni coatings at 0.1–2 keV

I. V. Kozhevnikov,[a]* E. O. Filatova,[b] A. A. Sokolov,[b,c] A. S. Konashuk,[b] F. Siewert,[c] M. Störmer,[d] J. Gaudin,[e] B. Keitel,[f] L. Samoylova[g] and H. Sinn[g]

[a]Shubnikov Institute of Crystallography, Russian Academy of Sciences, Leninsky Prospect 59, Moscow 119333, Russian Federation, [b]St Petersburg State University, Ulyanovskaya 3, Peterhof, St Petersburg 198504, Russian Federation, [c]Helmholtz-Zentrum Berlin für Materialien und Energie GmbH, Albert Einstein Strasse 15, 12489 Berlin, Germany, [d]Helmholtz-Zentrum Geesthacht, Institute of Materials Research, Max-Planck-Strasse 1, 21502 Geesthacht, Germany, [e]Université Bordeaux 1, CEA, CNRS, CELIA, 351 Cours de la Libération, 33405 Talence, France, [f]DESY, Notkestrasse 85, 22607 Hamburg, Germany, and [g]European XFEL GmbH, Albert Einstein Ring 19, 22761 Hamburg, Germany. *E-mail: ivk@crys.ras.ru

The use of soft X-rays near the carbon edge of absorption (270–300 eV) greatly enhances studies in various branches of science. However, the choice of reflecting coatings for mirrors operating in free-electron and X-ray free-electron laser (FEL and XFEL) beamlines in this spectral range is not so evident and experimental justifications of the mirror efficiency are rather limited. In the present paper it is demonstrated experimentally that the reflectivity of B_4C- and Ni-coated grazing-incidence mirrors is high enough for their operation in FEL or XFEL beamlines near the carbon *K*-edge of absorption. The minimal reflectivity of both mirrors proves to exceed 80% near the carbon absorption edge at a grazing angle of 0.6°. An in-depth profile of the chemical elements composing the reflecting coatings is reconstructed based on analysis of a set of reflectivity curves measured *versus* the grazing angle at different photon energies in the soft X-ray spectral region. This allows us to predict correctly the mirror reflectivity at any X-ray energy and any grazing angle.

Keywords: soft X-ray optics; XFEL mirrors; inverse problem; in-depth profile.

1. Introduction

The need for minimizing damage of the mirrors in free-electron and X-ray free-electron laser (FEL and XFEL) beamlines requires extremely small grazing angles of the incident radiation and the use of a light material (such as C, B_4C, B) as a reflecting coating of the mirror (Hau-Riege *et al.*, 2010; Chalupský *et al.*, 2009). Among them, C and B_4C appear to be more preferable from a technological point of view since they possess a very high sublimation and melting point, respectively. Using soft X-rays near the carbon edge (270–300 eV) greatly enhances the study of biological objects (Kirz *et al.*, 1995) and soft matter (Ade, 2012), which consist primarily of carbon and other elements with small *Z*, and characterization of organometallic molecules and carbon-based materials (Minasian *et al.*, 2013), in which the physics and chemistry of many important processes are determined by the electronic structure of chemical bonds of light atoms (C, N and O).

However, the polarizability of carbon atoms decreases sharply near the carbon *K*-edge of absorption and even changes its sign, so that the phenomenon of total external reflection of soft X-rays from carbon coating disappears. As a result, a sharp decrease in the reflectivity of the carbon-coated mirror is observed near the *K*-edge of absorption. Evidently, the presence of carbon in B_4C coating results in a reflectivity decrease near the carbon *K*-edge as well. Note that the situation is dramatized by the fact that any surface, while it is placed in vacuum, is covered by an adhesive contamination layer consisting mainly of molecules of hydrocarbons and water. This means that a decrease in the reflectivity near the carbon and oxygen *K*-edges will be observed for any mirror coating. At the same time, as the carbon concentration is lower, we can expect that the reflectivity decrease of B_4C- and Ni-coated mirrors is essentially weaker. In the present paper we demonstrate experimentally that the reflectivity of B_4C- and Ni-coated grazing-incidence mirrors is high enough for their operation in FEL or XFEL beamlines near the carbon *K*-edge of absorption. The minimal reflectivity of both mirrors proves to exceed 80% near the carbon absorption edge at a grazing angle of 0.6°. Both coating materials are therefore good alternatives to the standard coating material of amorphous carbon (a-C).

To predict the mirror reflectivity at arbitrary photon energy and grazing angle it is necessary to know the in-depth profile of all chemical elements of the reflecting coating. Studying the internal structure of the mirrors, which is based on analysis of reflectivity curves measured *versus* the grazing angle at different X-rays energies, is discussed in this paper as well.

2. Experimental

Carbon, boron carbide and nickel films of thickness 47–49 nm were coated on well polished monocrystalline silicon substrates (100 mm × 20 mm × 30 mm) in the HZG magnetron sputtering facility with a deposition length of up to 1.5 m (Störmer *et al.*, 2010, 2011). The ultrahigh-vacuum chamber was evacuated to a base pressure of less than 10^{-7} mbar, and the Ar working pressure was 0.002 mbar. The generator powers were 400 W DC, 600 W MF (medium frequency) and 120 W DC for C, B_4C and Ni coatings, respectively. It is possible to coat uniform thick and graded single layers due to the movement of the sample in front of the sputtering source. Moreover, this procedure could also be repeated with two sources in order to achieve multilayer mirrors.

Reflectivity measurements in the soft X-ray (SXR) region were performed using *s*-polarized synchrotron radiation in the reflectometer setup on the optics beamline (D-08-1B2) at the BESSY II storage ring of the Helmholtz-Zentrum Berlin (BESSY, 2014*a*,*b*). The energy resolution was about $E/\Delta E$ = 5000 and the accuracy of the energy scale was 10 meV. All curves discussed below were measured with an angular accuracy of 0.001°. A GaAsP diode, together with a Keithley electrometer, was used as a detector. The entrance aperture of the detector was wide enough (4 mm) to collect the total reflected radiation including both the scattered and the specularly reflected one.

In the working energy range from 35 eV to 700 eV, where the presence of higher diffraction orders cannot be avoided just by operation with a plane-grating monochromator in low C_{ff}-factors mode, a set of filters (Al, Be, B, C_6H_8, Ti and Fe) was used. For a good balance between transmission and suppression efficiency the filters thickness was 750 nm except for the Al (500 nm) and C_6H_8 (1500 nm) filters. A suppression factor of order 1000–10 was reached by using a transmission cut-off at the absorption edges for photons with twice the energy of the first-order one.

Two types of measurements were performed: (i) reflectivity $R(\theta)$ *versus* grazing angle at four different photon energies E = 140, 260, 450 and 650 eV for the C and B_4C coatings and E = 140, 450, 650 and 900 eV for the Ni coating, and (ii) spectral dependencies of the reflectivity $R(E)$ including relevant absorption edges at three grazing angles $\theta = 0.6°$, 1.2° and 1.8°; these values are typical for application of mirrors in FEL and future X-ray FEL beamlines.

The experimental reflectivity of the C-coated mirror measured *versus* the soft X-ray photon energy at three small grazing angles is shown by the solid curves in Fig. 1(*a*). A sharp variation in the reflectivity is clearly observed near the carbon and oxygen *K*-edges of absorption indicated by arrows in the figure. The availability of oxygen can be most likely explained by the presence of an adhesion layer always forming on any surface and consisting mainly of hydrocarbons and water molecules.

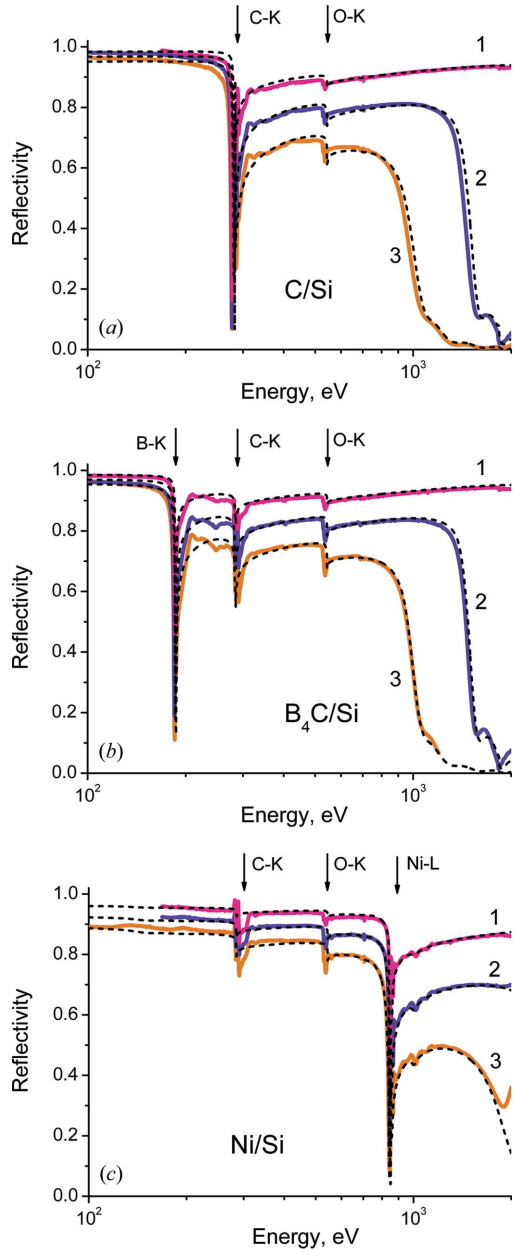

Figure 1
Experimental reflectivities (solid curves) of C-coated (*a*), B_4C-coated (*b*) and Ni-coated (*c*) mirrors *versus* the soft X-ray photon energy at three different grazing angles $\theta = 0.6°$ (1), 1.2° (2) and 1.8° (3). Dashed curves were calculated without a fitting procedure with the use of the atomic concentration profiles shown in Figs. 3(*a*), 4(*a*) and 5(*a*). Arrows indicate the position of the boron, carbon, oxygen and nickel *K*- and *L*-edges of absorption.

Fig. 1(*a*) demonstrates clearly that the reflectivity of the C-coated mirror decreases drastically near the carbon *K*-edge of absorption resulting in the impossibility of its use in FEL/XFEL beamlines in this spectral range. In fact, the real part of the dielectric constant of carbon exceeds unity near the *K*-edge of absorption (Henke *et al.*, 1993, 2014), while in a rather

narrow spectral interval, and absorption (the imaginary part of the dielectric constant) increases by more than 20 times with energy passing through the *K*-edge of absorption at $E \simeq 280$ eV. Therefore, the effect of total external reflection disappears here resulting in a reflectivity drop even at small grazing angles of an incident beam. The deepest reflectivity drop is observed at the photon energy $E \simeq 277.6$–278.6 eV, where the reflectivity falls down to 16.3% at $\theta = 0.6^\circ$, 7.2% at $\theta = 1.2^\circ$ and 6.8% at $\theta = 1.8^\circ$.

The effect of the carbon *K*-edge on the reflectivity of the B_4C-coated mirror is essentially weaker because of the relatively low content of carbon atoms in boron carbide. Experimental justification of this conclusion is illustrated in Fig. 1(*b*), where the measured reflectivity (solid curves) of the B_4C-coated mirror is shown *versus* the photon energy at the same grazing angles as above. In contrast to the C-coated mirror the deep drop in the reflectivity is observed near the boron *K*-edge of absorption. However, the reflectivity drop near the carbon *K*-edge is essentially lower compared with the C-coated mirror: the reflectivity of the B_4C mirror falls down to only 80.9% at $\theta = 0.6^\circ$, 67.8% at $\theta = 1.2^\circ$ and 56.4% at $\theta = 1.8^\circ$. The reflectivity minimum is observed at a soft X-ray energy of about 290.6–290.7 eV. As in the case of the C-coated mirror the oxygen *K*-edge of absorption is traced in the measured reflection spectrum. Since B_4C is a stable chemical compound the most plausible explanation of the availability of oxygen is the presence of an adhesion layer on the sample surface.

Finally, the reflectivity of the Ni-coated mirror is shown in Fig. 1(*c*) as a function of the photon energy at three different grazing angles. A deep drop in the reflectivity is observed near the Ni $L_{2,3}$-edge of absorption. In addition, minima of the reflectivity are clearly seen at photon energies near the *K*-edges of absorption of oxygen and carbon, while the last element is not contained in the Ni film. As above, these minima are caused by an adhesion layer placed on top of the sample and, in addition, by a native oxide layer (NiO) on top of the Ni film. The reflectivity minimum near the C-edge of absorption is observed at a soft X-ray energy of $\sim$290.7 eV independently of the grazing incident angle. Its value is equal to 83.8% at $\theta = 0.6^\circ$, 79.9% at $\theta = 1.2^\circ$ and 73.0% at $\theta = 1.8^\circ$.

Thus, the B_4C- and Ni-coated mirrors were demonstrated experimentally to be quite acceptable for operation in FEL/XFEL or synchrotron beamlines near the carbon *K*-edge of absorption.

3. Depth profile analysis of the coating layers

To explain the observed spectral dependence of the reflectivity and to predict the reflectivity of the mirrors at arbitrary soft X-ray energy and grazing angle, it is necessary to develop an adequate model of the reflecting coatings, namely to determine the depth-distribution of concentration of the chemical elements in the samples. Then we can calculate the depth-distribution of the complex dielectric constant $\varepsilon(z,E)$ and, hence, the reflectivity of the mirrors at any X-ray energy and grazing angle.

The reflectivity of a layered sample is determined entirely by the depth-distribution of the matter polarizability $\chi(z, E) \equiv 1 - \varepsilon(z, E)$ depending on the photon energy *E*. If the sample consists of several chemical elements $A, \ldots, B$, the matter polarizability in the soft X-ray region can be represented as a linear combination of polarizabilities of individual atoms,

$$\chi(z, E) \simeq E^{-2}\left[C_A(z) f_A(E) + \ldots + C_B(z) f_B(E)\right], \qquad (1)$$

where $C_j(z)$ and $f_j(E)$ are the atomic concentration profile and the complex atomic scattering factor of the *j*th element, respectively, and the values of $\mathrm{Re}(f)$ and $\mathrm{Im}(f)$ characterize refraction and absorption of the soft X-ray radiation, respectively. The values of $f_j(E)$ as a function of energy for all chemical elements can be found elsewhere; for example, at the web site of the Center for X-ray Optics (Berkeley) (Henke *et al.*, 2014).

The atomic scattering factor $f_j(E)$ is changed essentially with the photon energy passing through the absorption edge, and, hence, the contribution of an individual chemical element to the total polarizability (1) is distinct at different energies. Thus, by analyzing a set of reflectivity curves measured at different photon energies we can attempt to deduce the concentration profiles $C_j(z)$ of all the chemical elements in the sample. A detailed discussion of the approach, several examples of the reconstructed concentration profiles of layered samples, and a comparison of the results with those obtained by photoelectron spectroscopy and transmission electron microscopy are given by Filatova *et al.* (2009, 2012*a*,*b*).

There are a large amount of papers where the analysis of the internal structure of a sample is based on the reflectivity measurements at different photon energies including near the absorption edge of a studied chemical element (see, for example, Tonnerre *et al.*, 1998; Wang *et al.*, 2007; Kemik *et al.*, 2011; Nayak & Lodha, 2013, and references therein). Such an approach is very sensitive to the presence of the element at even very low concentration. However, the polarizability (atomic scattering factor) of the element near the absorption edge is unknown, because it depends essentially on the chemical bonds in the substance. As an example, the polarizability of carbon atoms near the absorption edge may be quite different for atoms in the reflecting coating (C or B_4C) and in the adhesion layer. Therefore, in parallel to the reconstruction of the in-depth profile of the atomic concentrations, it is necessary to determine the complex scattering factors of carbon in both materials. As a result, the problem of ambiguity of the inverse problem solution becomes essentially more difficult.

In contrast, in our approach the wavelength of a probing beam is not very close to the absorption edges of the chemical elements studied, so that we can use data presented in the Henke table (Henke *et al.*, 2014). An example of the reflectivity curves measured *versus* the grazing angle at four different photon energies lying between absorption edges is shown in Fig. 2 (circles) for the Ni-coated mirror.

First of all, we performed a conventional fit to the experimental reflectivities of C and B_4C mirrors in frames of the trilayer model of the samples AdL/coating/SiO_2/Si taking into

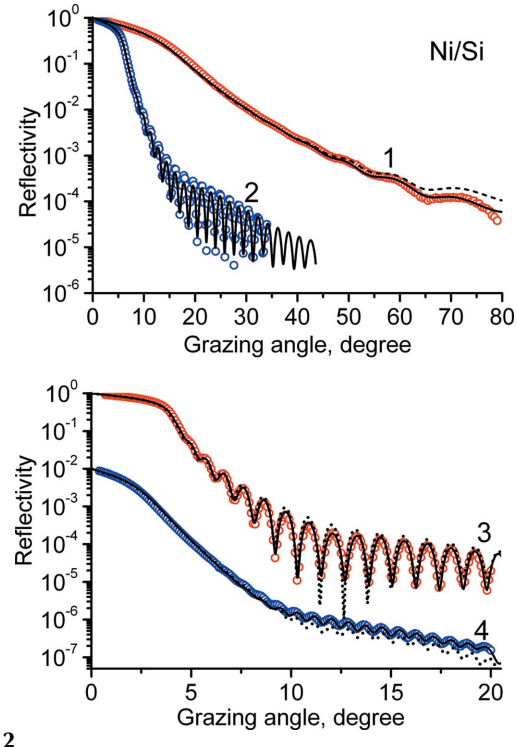

Figure 2
Experimental reflectivity (circles) of the Ni-coated mirror *versus* the grazing angle in the soft X-ray region at photon energies E = 140 eV (1), 450 eV (2), 650 eV (3) and 900 eV (4). Dashed curves are the result of calculation in frames of the four-layer model with the use of the concentration profiles shown in Fig. 5(*a*). Solid curves were obtained after numerical refinement and were calculated with the use of the depth-distribution of the chemical elements concentration shown in Fig. 5(*b*). Curve 4 is shifted down by a factor of 100 for clarity.

account both an oxide layer on top of the Si substrate and an adhesion layer (AdL) on top of the film. The tri-layer model proves to be unable to describe properly the experimental reflectivity curves of the Ni-coated mirror. Therefore, we use a more complex four-layer model of the mirror, AdL/NiO/Ni/SiO_2/Si, introducing an oxide layer on top of the Ni film. All four experimental reflectivity curves $R(\theta,E)$ were processed simultaneously for each sample. The fitting parameters were the film thickness and density of all the layers as well as the interface width between neighbouring materials, where the dielectric constant is assumed to follow the error function. The silicon density (2.33 g cm^{-3}) in the depth of the substrate is supposed to be known. The stoichiometry of the adhesion layer is expected to be C + $x$$H_2O$ (hydrocarbons and water), where x a further fitting parameter.

The necessity of introducing an adhesion layer on the internal sample surface and an oxide layer on top of the substrate into the film model was discussed and analyzed by Filatova *et al.* (2009, 2012*a*,*b*), where the impossibility of an adequate description of experimental reflectivities was demonstrated if these layers were neglected.

The fitting results shown in Fig. 2 (dashed curves) demonstrate that the simplest model of the samples allows us to describe reasonably the experimental reflectivity curves, while a certain disagreement between the measured and calculated curves is still observed. The depth distributions of the chemical elements concentration shown in Figs. 3(*a*), 4(*a*) and 5(*a*) look quite reasonable as well. The film densities are equal to 2.18 (C), 2.39 (B_4C) and 8.31 (Ni) g cm^{-3}, which are about 0.93 (Ni), 0.95 (B_4C) and 0.99 (C) of the bulk density. A slight reduction in the film density is typical for magnetron sputtering. The adhesion layer on the sample top is thin (1.5–2.4 nm thickness) and loose (maximum density 1.3–1.5 g cm^{-3}), its density being decreasing gradually into vacuum. The parameter x characterizing the stoichiometry of the adhesion layer (C + $x$$H_2O$) proves to be equal to 0.3–0.4. The maximal density of the nickel oxide layer on top of the Ni film is equal to 7.30 g cm^{-3}, its thickness is about 4 nm, and the oxygen concentration decreases gradually into the depth of the Ni film. The interface width of the external film surface is found to be 1.05 (C), 0.50 (B_4C) and 0.56 (Ni) nm. These values agree well with the values of the root-mean-squared roughness obtained by the atomic force microscopy (2 × 2 µm scan): σ = 1.03 ± 0.05, 0.52 ± 0.05 and 0.49 ± 0.05 nm for the C-, B_4C- and Ni-coated mirror, respectively, the σ-values changing slightly over the surface.

The main problem of the concentrations or dielectric constant profile reconstruction is connected to its ambiguity, *i.e.* to a lot of local minima of the merit function, even though a simple model of the sample is used (Volkov *et al.*, 2013). To choose uniquely the solution corresponding to reality, we compared the fine structure of the interlayer on top of the Si substrates. As the substrates were identical in our experi-

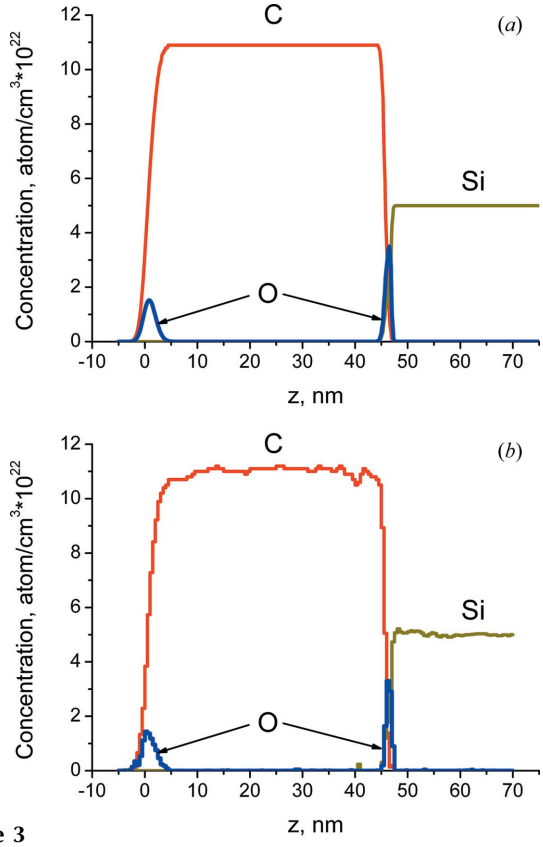

Figure 3
Depth-distribution of the concentration of the chemical elements in the C-coated mirror found in frames of the tri-layer model (*a*) and after numerical refinement (*b*). The z-axis is directed into the substrate.

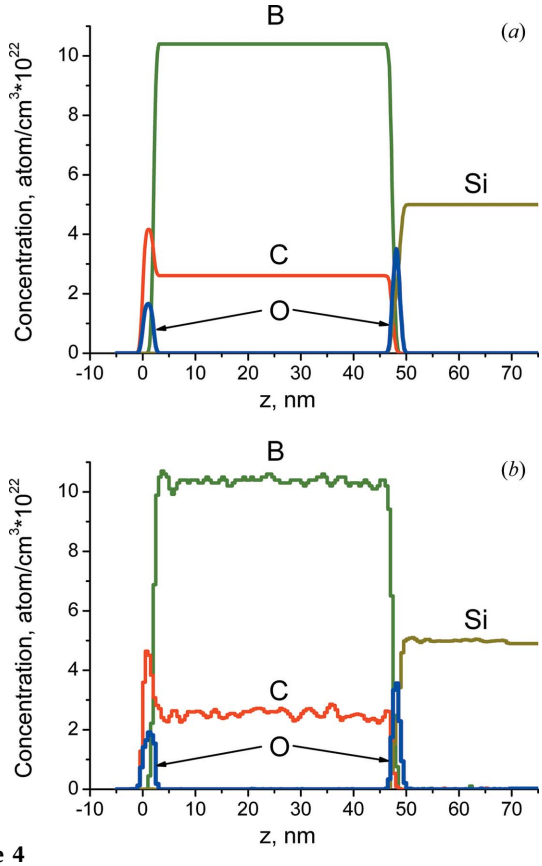

Figure 4
Depth-distribution of the concentration of the chemical elements in the B_4C-coated mirror found in frames of the tri-layer model (*a*) and after numerical refinement (*b*). The *z*-axis is directed into the substrate.

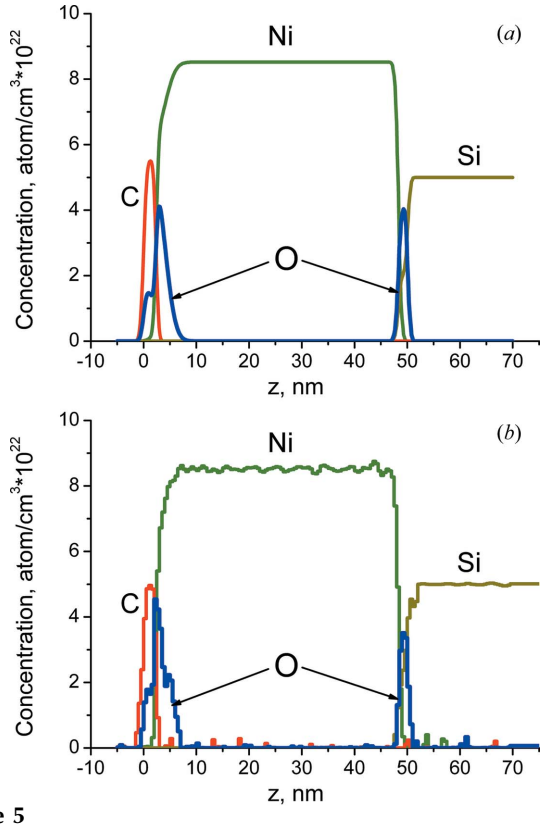

Figure 5
Depth-distribution of the concentration of the chemical elements in the Ni-coated mirror found in frames of the four-layer model (*a*) and after numerical refinement (*b*). The *z*-axis is directed into the substrate.

ments, it should be the same for all the samples studied. Indeed, the concentration profiles shown in Figs. 3(*a*), 4(*a*) and 5(*a*), and chosen just as a result of a comparison of the substrate parameters, demonstrate practically identical values of the density of the silicon oxide layer on the substrate top (2.05 ± 0.05 g cm^{-3}), its thickness (1.6 ± 0.2 nm at the half of the height of oxygen concentration peak) and the root-mean-squared roughness of the substrate (0.40 ± 0.05 nm).

To check the validity of the found concentration profiles we calculated the reflectivity curves $R(E)$ *versus* the photon energy. Results of the calculation are shown in Fig. 1 (dashed curves). During the calculation, the concentration profiles shown in Figs. 3(*a*), 4(*a*) and 5(*a*) were used and no additional fitting procedure was performed. As seen, the calculated reflectivities of the C and B_4C mirrors agree almost ideally with the experimental curves except for narrow spectral intervals near the absorption edges. Even small features on the reflectivity curves 2 and 3 observed at a photon energy of the order of 1–2 keV and caused by reflection from the substrate are properly described.

Agreement between the calculated and experimental reflectivities is somewhat poorer for the Ni-coated mirror (Fig. 1*c*). The model developed is unable to explain the appearance of the feature (local minimum) on the reflectivity curve 3 at $E \simeq 2$ keV. Moreover, the depth of the reflectivity minima near the edges of absorption is essentially smaller compared with the experimental data. Probably, the internal structure of the Ni coating is more complex compared with the four-layer model used.

The next step of analysis consisted of the numerical refinement of the model solutions to describe quantitatively all features observed in the measured reflectivity curves $R(\theta)$. We used the refinement procedure based on the conception of maximum entropy, which was used earlier by Filatova *et al.* (2009, 2012*a*,*b*) to process the reflectivity curves measured in the soft X-ray region.

The generalized Shannon–Jaynes entropy S (negative function) is given by Skilling (1988),

$$S = \sum_{i,j} \left\{ C_j(z_i) - C_j^{(0)}(z_i) - C_j(z_i) \log\left[C_j(z_i)/C_j^{(0)}(z_i) \right] \right\} \quad (2)$$

where $C_j(z_i)$ is the concentration of jth element in the ith pixel of the digitized reconstruction of $C_j(z)$, and $C_j^{(0)}(z)$ is a default model with respect to which the entropy is measured. In our case, $C_j^{(0)}(z)$ is the solution of the problem found in the frames of the three- or four-layer model. If we put $C_j(z) = C_j^{(0)}(z)$, the entropy is equal to zero. The method is based on the determination of solution $C_j(z)$ providing the necessary accuracy to fit the experimental reflectivity curves and, simultaneously, the maximum entropy, *i.e.* on the determination of a solution 'closest' to the default one.

The fitting accuracy is illustrated by solid curves in Fig. 2 and the refined concentration profiles are shown in Figs. 3(*b*),

4(*b*) and 5(*b*). As can be seen, very small deformation of the concentration profiles allowed us to describe all the experimental curves with very high accuracy. It is probable that small-scale oscillations on the profiles have no physical sense, as was discussed by Filatova *et al.* (2012*a*, 2012*b*). A slight deformation of the interfaces between neighbouring films is more important as it can result in an essential change of the reflectivity curve.

The refined film models result in practically the same reflectivities calculated as a function of the photon energy at small grazing angles and, therefore, are not shown in Fig. 1.

4. Summary and conclusions

We have demonstrated experimentally the possibility to use a B_4C-coated mirror near the carbon edge of absorption. The minimal value of the mirror reflectivity near the carbon absorption edge is rather high and achieves 80.9% at the grazing angle $\theta = 0.6^\circ$, 67.8% at $\theta = 1.2^\circ$ and 56.4% at $\theta = 1.8^\circ$.

We studied the in-depth profiles of the chemical elements composing the reflecting coatings of FEL/XFEL mirror prototypes. The approach is based on analysis of the reflectivity curves measured as a function of the grazing angle at different X-rays energies. Knowing the in-depth profile we can predict the mirror reflectivity at any X-ray energy and at any incidence angle. It would be interesting to use the same method for analysis of the long-term variation of the internal structure and stability of the reflecting coatings under their operation in FEL/XFEL beamlines.

One of the authors (IVK) was supported by the Russian Ministry of Science and Education *via* the program 'Physics at the accelerators and reactors of West Europe (excluding CERN)'.

References

Ade, H. (2012). *Eur. Phys. J.* **208**, 305–318.
BESSY (2014*a*). *Optics beamline*, http://www.bessy.de/bit/upload/D081B2.pdf.
BESSY (2014*b*). *Reflectometer station*, http://www.bessy.de/bit/upload/reflectometer.pdf.
Chalupský, J., Hájková, V., Vyšín, L., Burian, T., Juha, L., Altapova, V., Sinn, H., Tschentscher, Th., Jurek, M., Sobierajski, R., Wabnitz, H., Toleikis, S., Tiedtke, K., Störmer, M., Gleeson, A. J. & Gaudin, J. (2009). *Appl. Phys. Lett.* **95**, 1111–031111.
Filatova, E. O., Kozhevnikov, I. V., Sokolov, A. A., Ubiyvovk, E. V., Yulin, S., Gorgoi, M. & Schaefers, F. (2012*b*). *Sci. Technol. Adv. Mater.* **13**, 015001.
Filatova, E. O., Sokolov, A. A. & Kozhevnikov, I. V. (2012*a*). *High-k Gate Dielectrics for SMOS Technology*, edited by H. Gang, pp. 225–271. Weinheim: Wiley-VCH Verlag.
Filatova, E. O., Sokolov, A. A., Kozhevnikov, I. V., Taracheva, E. Yu., Grunsky, O. S., Schaefers, F. & Braun, W. (2009). *J. Phys. Condens. Matter*, **21**, 185012.
Hau-Riege, S. P., London, R. A., Graf, A., Baker, S. L., Soufli, R., Sobierajski, R., Burian, T., Chalupsky, J., Juha, L., Gaudin, J., Krzywinski, J., Moeller, S., Messerschmidt, M., Bozek, J. & Bostedt, C. (2010). *Opt. Express*, **18**, 23933–23938.
Henke, B. L., Gullikson, E. M. & Davis, J. C. (1993). *At. Data Nucl. Data Tables*, **54**, 181–342.
Henke, B. L., Gullikson, E. M. & Davis, J. C. (2014). *X-ray Database of X-ray Interactions with Matter*, http://henke.lbl.gov/optical_constants/.
Kemik, N., Gu, M., Yang, F., Chang, C.-Y., Song, Y., Bibee, M., Mehta, A., Biegalski, M. D., Christen, H. M., Browning, N. D. & Takamura, Y. (2011). *Appl. Phys. Lett.* **99**, 201908.
Kirz, J., Jacobsen, C. & Howells, M. (1995). *Q. Rev. Biophys.* **28**, 33–130.
Minasian, S. G., Keith, J. M., Batista, E. R., Boland, K. S., Kozimor, S. A., Martin, R. L., Shuh, D. K., Tyliszczak, T. & Vernon, L. J. (2013). *J. Am. Chem. Soc.* **135**, 14731–14740.
Nayak, M. & Lodha, G. S. (2013). *J. Appl. Cryst.* **46**, 1569–1575.
Skilling, J. (1988). *Maximum Entropy and Bayesian Methods.* Cambridge/Amsterdam: Kluwer.
Störmer, M., Horstmann, C., Siewert, F., Scholze, F., Krumrey, M., Hertlein, F., Matiaske, M., Wiesmann, J. & Gaudin, J. (2010). *AIP Conf. Proc.* **1234**, 756–759.
Störmer, M., Siewert, F. & Gaudin, J. (2011). *Proc. SPIE*, **8078**, 80780G.
Tonnerre, J. M., Sève, L., Barbara-Dechelette, A., Bartolomé, F., Raoux, D., Chakarian, V., Kao, C. C., Fischer, H., Andrieu, S. & Fruchart, O. (1998). *J. Appl. Phys.* **83**, 6293–6295.
Volkov, Yu. O., Kozhevnikov, I. V., Roshchin, B. S., Filatova, E. O. & Asadchikov, V. E. (2013). *Crystallogr. Rep.* **58**, 160–167.
Wang, Ch., Araki, T., Watts, B., Harton, S., Koga, T., Basu, S. & Ade, H. (2007). *J. Vac. Sci. Technol. A*, **25**, 575–586.